Discussing 125 GeV and 95 GeV excess in light radion model

Divya Sachdeva[1,*] and Soumya Sadhukhan[2,†]

[1]*Department of Physics, Indian Institute of Science Education and Research Pune, Pune 411008, India*
[2]*Department of Physics and Astrophysics, University of Delhi, Delhi 110 007, India*

(Received 7 September 2019; accepted 19 February 2020; published 31 March 2020)

Even if the LHC observations are consistent with the Standard model (SM), current LHC results are not precise enough to rule out the presence of new physics. Taking a contrarian view of the SM Higgs fandom, we look out for a more suitable candidate for the 125 GeV boson observed at the LHC. At the same time, a recent result from CMS hints toward an excess near 95 GeV in the diphoton ($\gamma\gamma$) channel. Given these aspects, we revisit the Higgs-radion mixing model to explore the viability of the radion mixed Higgs to be the 125 GeV boson along with the presence of a light radion (to be precise, Higgs mixed radion) that can show up in future experiments in the $\gamma\gamma$ channel. We find that the mixed radion-Higgs scenario gives a better fit than the SM, with the radion mixed Higgs as a more suitable 125 GeV scalar candidate. It also gives rise to a diphoton excess from the light radion, consistent with the LHC observations.

DOI: 10.1103/PhysRevD.101.055045

I. INTRODUCTION

The discovery of a boson of mass 125 GeV at the LHC validates the Standard Model to be the most predictive model of particle physics. As LHC probes the boson further, it turns out that its interactions match the Standard Model (SM) Higgs boson, albeit with minor exceptions. Still, the debate if the SM is the ultimate theory of the particle world is far from over, and LHC results with large uncertainties can disclose new possibilities. The current measurement of the Higgs signal strengths [1–3] still allow for small yet significant deviation from the SM values. Therefore, it is worthwhile to look for a more suitable Higgs candidate than the SM Higgs, which can be explored in different beyond the Standard model (BSM) scenarios. As the LHC observations indicate the presence of a scalar that mimics the SM Higgs, only a model with minimal modification in the scalar sector is likely to accommodate a more interesting alternative. As we invoke BSM scenarios containing a Higgs-like scalar, it would be interesting if these can also address the issues plaguing the SM, viz., the resolution of the gauge hierarchy problem, an explanation of the baryon asymmetry, offering a dark matter candidate, etc.

Even after the 8 and 13 TeV run of the LHC with increasing luminosities, any trace of new physics at the TeV scale that can potentially fix the gauge hierarchy problem is yet to be discovered. If this is taken to imply that new physics exists only at energies higher than the TeV scale, a little fine-tuning is automatically introduced. It can be avoided if the new physics search is concentrated around the Higgs mass scale. Furthermore, it is quite conceivable that the new physics can be hidden at a lower scale, i.e., lighter than the Higgs, instead of always at a scale higher (approximately TeV). Especially in the hadron colliders like the LHC, probing the lighter spectrum is not that efficient due to enormous QCD background. Therefore, it is pertinent to consider innovative model construction aided by enhanced signal strength where BSM physics can be probed at the sub-100-GeV scale. Another recent motivation that prods us to probe at lower scales is the variety of mild excesses we have observed over the years [4–6]. Among these observations, the most recent result from CMS [7] shows a small excess near 95 GeV in the diphoton channel. All of these observations compel us to look out for the new physics models at these scales carefully, especially the one where diphoton resonance can be an important feature.

To arrange for a better 125 GeV Higgs-like candidate along with a light spectrum, extended scalar sector BSM scenarios can be delved into. While a new scalar discovery in future experiments will compel us to explore beyond minimal Higgs sector of the SM, the 125 GeV particle as the only observed scalar can also have an underlying extended scalar sector. The simplest extension of the SM scalar sector is to add a singlet scalar. However, as it mixes minimally with the Higgs, it is unable to give rise to an

*divyasachdeva951@gmail.com
†physicsoumya@gmail.com

excess in the diphoton channel over other channels and is, therefore, of no major interest for this work. The Higgs sector extended with another $SU(2)_L$ doublet, motivated by the supersymmetric and grand unified theories, also severely constrains the presence of a light scalar due to the sum rule of scalar couplings to fermions and gauge bosons, as discussed in Ref. [8]. In this regard, the radion, a scalar introduced in extra-dimensional model to stabilize the geometry, is discussed. Being the Goldstone boson of the scale invariance breaking, it has trace anomaly-induced couplings to the massless bosons (photons as well as gluons) and consequently allows for a distinct possibility of a nontrivial diphoton decay. Contrary to the other BSM scalars, it can be really light with mass approximately 100 GeV as had been shown in the Randall-Sundrum (RS) model [9–11]. In addition, it can mix to the Higgs boson via curvature scalar mixing, and this can alter the Higgs couplings significantly. Therefore, it behoves us to probe radion-Higgs mixing scenario to assess the viability of a nonstandard Higgs as the 125 GeV scalar at the LHC.

The radion Higgs mixing as has been explored later in our work can significantly modify the couplings of both the scalar mass eigenstates. More specifically, the Higgs gluon-gluon coupling is enhanced due to the contribution from the trace anomalous part of the radion gluon-gluon vertex, which is found to help explain the signal strength of the Higgs signal better than the SM Higgs itself. The significant parameter region where the radion mixed Higgs is a more suitable candidate for the 125 GeV boson instead of the SM Higgs hitherto pitched so aggressively is presented. If we explore the lighter than 125 GeV side of the spectrum in the context of a diphoton excess, the RS model radion can be a suitable candidate. The radion gamma-gamma vertex is modified compared to that of a SM-like Higgs due to its trace anomaly part, and this can increase its branching ratio to the diphoton channel with respect to the other fermionic and gauge boson channels. Therefore, it is worthwhile to propose the radion as a natural candidate that can potentially give rise to the diphoton excess.

While some of the observations in this paper have already been noted in the previous works [12–15] and the diphoton excess due to the light scalar has also been discussed in several papers [16–31], the data used are current, leading to new bounds, and we show that the extension of SM by such a scalar can actually give a better fit to the Higgs signal measurement. We begin our discussion with a short review on the radion in the RS model so that this paper can be read as far as possible independently of the preceding literature. Next, in Sec. III, we discuss phenomenological and theoretical constraints on parameter space of the radion and then show, in Sec. IV how the new scalar may explain the recent CMS excess near 95 GeV, as well as give the better fit to the Higgs signal measurement. We conclude in Sec. V.

II. MODEL DESCRIPTION

We first introduce the minimal RS model and show how the radion can appear here, outlining its interaction with the SM particles. Then, we analyze radion Higgs mixing through scalar-curvature interaction, listing the modified couplings for both the scalars.

A. Minimal RS model

In the minimal version of the RS model, an extra warped dimension of radius r_c is compactified down to a S_1/Z_2 orbifold. The orbifolding is applied with a pair of 3-branes at the fixed points $x_4 = 0$ and $x_4 = r_c\pi$. The brane at $x_4 = 0$, where gravity peaks, is called the Planck (hidden) brane, while the brane where SM fields are confined is called the TeV (visible) brane. Note that there are many other versions of the model where fields other than the graviton are allowed to propagate in the bulk; however, we limit ourselves to the minimal case. The action for this set up is given by [32]

$$\begin{aligned} S &= S_{\text{gravity}} + S_v + S_h \\ S_{\text{gravity}} &= \int d^5x\sqrt{-g}\{2M_5^3R - \Lambda\} \\ S_v &= \int d^4x\sqrt{-g_v}\{\mathcal{L}_v - V_v\} \\ S_h &= \int d^4x\sqrt{-g_h}\{\mathcal{L}_h - V_h\}, \end{aligned} \tag{1}$$

where g is the determinant of the five-dimensional metric $g_{MN}(x_\mu, x_4)$, the greek indices being representations of $(1+3)$-dimensional coordinates on the visible (hidden) brane, and M_5 is the five-dimensional (5D) Planck mass, and Λ is the bulk cosmological constant. V_v and V_h are the brane tensions of visible and hidden branes, respectively.

After solving Einstein's equations, the metric has the form

$$ds^2 = e^{-2k|x_4|}\eta_{\mu\nu}dx^\mu dx^\nu + dx_4^2, \tag{2}$$

where $k = \sqrt{\frac{-\Lambda}{24M_5^3}}$, $V_h = -V_v = 24M_5^3k$, $|x_4| = r_c\phi$ (ϕ being the angular coordinate). M_5 is related to the four-dimensional Planck mass, M_{Pl}, as

$$M_{\text{Pl}}^2 = \frac{M_5^3}{k}[1 - e^{-2kr_c\pi}]. \tag{3}$$

A field with mass m propagating on the visible brane in the five-dimensional theory generates an effective mass $m_{\text{eff}} = me^{-kr_c\pi}$ in the four-dimensional (4D) effective theory. To solve the hierarchy problem, one needs $kr_c \sim 12$. With this value, the Planck scale is reduced to the weak scale. However, for the background metric solution discussed above, any value of the radius r_c is equally possible. Therefore, a mechanism is needed to fix it uniquely with the desired value so that the EW hierarchy can be

explained. One of the mechanisms [9,33–35] that addresses this issue was given by Goldberger and Wise (GW) [9].

In the GW mechanism, r_c is considered as the vacuum expectation value (vev) of a modulus field $F(x)$ that quantifies the fluctuation about the radius:

$$ds^2 = e^{-2k|\theta|F(x)} g_{\mu\nu} dx^\mu dx^\nu - F^2(x) d\theta^2.$$

Upon reducing the 5D Einstein Hilbert action for this metric, the effective action is obtained,

$$\mathcal{S} = M_5^3 \int d^4x d\theta \sqrt{-g} e^{-2k\theta F(x)} (6k|\theta| \partial_\mu F(x) \partial^\mu F(x) - 6k^2 |\theta|^2 F \partial_\mu F(x) \partial^\mu F(x) + F(x) R), \tag{4}$$

where R is the 4D Ricci scalar. After we integrate out θ, we get the following 4D action for $\Phi = \sqrt{\frac{24M_5^3}{k}} e^{-k\pi F(x)}$:

$$\mathcal{S} = \frac{2M_5^3}{k} \int d^4x \sqrt{-g} \left[1 - \frac{k\Phi^2}{24M_5^3}\right] R + \frac{1}{2} \int d^4x \sqrt{-g} \partial_\mu \Phi \partial^\mu \Phi.$$

The vacuum expectation value, $\langle \Phi \rangle$, is obtained by introducing a bulk scalar with the interaction terms on both the branes. This bulk scalar then develops an effective 4D potential on the brane. The minimum of this potential can be arranged to yield the required value of kr_c as

$$\langle \Phi \rangle = \frac{24M_5^3}{k} e^{-k\pi r_c}. \tag{5}$$

The mass of the radion field about the minimum is given by

$$m_\Phi \sim \frac{kV_b}{2M_5^{3/2}} e^{-kr_c\pi}, \tag{6}$$

where V_b is the vev of the bulk stabilizing field on the hidden brane. It can be noticed that the precise mass of the radion is dependent on the backreaction. For small backreaction, the expression above dictates the radion mass to be of few hundreds GeV.

B. Radion couplings to SM fields

We expand Φ about its vev ($\langle \Phi \rangle$) as

$$\Phi = \langle \Phi \rangle + \varphi.$$

The interactions of the radion with matter on the visible brane can be written as

$$\mathcal{L}_{\text{int}} = \frac{\varphi}{\langle \Phi \rangle} (T^\mu_\mu) \equiv \frac{\varphi}{\Lambda_\varphi} (T^\mu_\mu), \tag{7}$$

where $\Lambda_\varphi \equiv \langle \Phi \rangle$, $T_{\mu\nu}$ is the symmetric and gauge invariant tree-level energy-momentum tensor, defined by

$$T_{\mu\nu} = \frac{2}{\sqrt{-g}} \frac{\delta \mathcal{S}_{\text{matter}}}{\delta g^{\mu\nu}}.$$

Restricting to interactions up to quadratic order in SM fields, the tree-level T^μ_μ has form

$$T^\mu_\mu = \sum_f \left(\frac{3}{2} \partial_\mu (\bar{f} i \gamma^\mu f) - 3 \bar{f} i \gamma^\mu \partial_\mu f + 4 m_f \bar{f} f \right) - \partial_\mu h \partial^\mu h + 2 m_h^2 h^2 - 2 m_W^2 W^{+\mu} W^-_\mu - m_Z^2 Z^\mu Z_\mu, \tag{8}$$

where the sum runs over all fermions f and h represents the Higgs boson. Note that the radion-SM coupling is exactly like the coupling of the Higgs boson, except that the SM vacuum expectation value v is replaced by Λ_φ. Hence, one expects radion phenomenology to be very similar to Higgs boson phenomenology. However, due to the trace anomaly, the gauge bosons have an additional interaction term

$$\mathcal{L}^{\text{gauge}}_{\text{int}} = \sum_i \frac{\beta(e_i)}{2e_i^3 \Lambda_\varphi} F^{\mu\nu i} F^i_{\mu\nu} \varphi, \tag{9}$$

where $\beta(e_i)$ is the beta function corresponding to the coupling e_i of the gauge field A_i. The sum is over all the gauge fields in the SM. Because of the anomaly term, the radion has sizable interaction strength with $\gamma\gamma$ and gg pairs, which are completely absent for the SM Higgs. For the case of W^+W^- and ZZ pairs, contribution due to the anomaly term is negligible compared to the corresponding terms in Eq. (9).

In addition to the above action, the radion-Higgs mixing scenario is also possible, and we review this in the next section.

C. Radion-Higgs mixing

Now, we discuss the mixed Higgs-radion scenario. This scenario has been discussed by several authors [12,36,37], with similar features, but here we choose to work with the formalism given in Refs. [12,37]. The results in Refs. [12,37] agree with Ref. [36] in the limit $\frac{v\xi}{\Lambda_\varphi} \ll 1$ with ξ being the mixing parameter.

The mixing is induced through the term

$$\mathcal{L}_{\text{mix}} = -\xi \sqrt{-g_i} R(g_i) H^\dagger H, \tag{10}$$

where $H = [0, (v+h)/\sqrt{2}]$ with $v = 246$ GeV and $g^i_{\mu\nu}$ is the induced metric. After expanding $\sqrt{-g_i} R(g_i)$ to linear order, we get

$$\mathcal{L}_{\text{mix}} = 6\xi\gamma h \Box \varphi + 3\xi\gamma^2 \partial_\mu \varphi \partial^\mu \varphi,$$

where $\gamma \equiv v/\Lambda_\varphi$. The first term induces kinetic mixing between the Higgs and radion, whereas the second term

modifies the kinetic term for the radion. The full Lagrangian including $\mathcal{L}_{\rm mix}$ becomes

$$\mathcal{L} = \frac{1}{2}\partial^\mu h \partial_\mu h - \frac{1}{2}m_h^2 h^2 + \frac{(1+6\gamma^2\xi)}{2}\partial^\mu\varphi\partial_\mu\varphi - \frac{1}{2}m_\varphi^2\varphi^2 - 6\gamma\xi\partial^\mu\varphi\partial_\mu h. \tag{11}$$

We first normalize the kinetic term using the transformations

$$h = h' + \frac{6\gamma\xi}{Z}\varphi', \qquad \varphi = \frac{\varphi'}{Z}, \tag{12}$$

where h', φ' are transformed fields, $Z^2 = 1 + 6\xi\gamma^2(1-6\xi)$, and Z^2 must be positive to get the real mixing matrix and thereby positive kinetic term. To diagonalize the mass matrix, the following orthogonal transformations are used,

$$h' = \cos\theta h_m + \sin\theta\varphi_m, \quad \varphi' = -\sin\theta h_m + \cos\theta\varphi_m, \tag{13}$$

such that

$$h = \left(\cos\theta - \frac{6\xi\gamma}{Z}\sin\theta\right)h_m + \left(\sin\theta + \frac{6\xi\gamma}{Z}\cos\theta\right)\varphi_m,$$
$$\varphi = -\frac{\sin\theta}{Z}h_m + \frac{\cos\theta}{Z}\varphi_m \tag{14}$$

where mixing angle θ is given as

$$\tan 2\theta = \frac{12\gamma\xi Z m_h^2}{m_\varphi^2 - m_h^2(Z^2 - 36\gamma^2\xi^2)}. \tag{15}$$

The real mixing angle keeps the radion kinetic term positive. This gives us a constraint on ξ:

$$\frac{1}{12}\left(1 - \sqrt{1+\frac{4}{\gamma^2}}\right) \le \xi \le \frac{1}{12}\left(1 + \sqrt{1+\frac{4}{\gamma^2}}\right).$$

The physical masses are given by

$$m_{\varphi_m}^2 = \frac{1}{2Z^2}(\Xi - \sqrt{\Xi^2 - 4Z^2 m_\varphi^2 m_h^2}) \tag{16}$$

$$m_{h_m}^2 = \frac{1}{2Z^2}(\Xi + \sqrt{\Xi^2 - 4Z^2 m_\varphi^2 m_h^2}), \tag{17}$$

where $\Xi = m_\varphi^2 + (1+6\gamma^2\xi)m_h^2$ and the sign is chosen so that the radion is lighter. From these formulas, it is clear that $\xi, m_h, m_\varphi, \Lambda_\varphi$ are unknown parameters. For our study, we trade m_h and m_φ in terms of the physical masses,

TABLE I. Coupling strength of the radion and Higgs with on-shell SM particles in the mixed radion-Higgs scenario in units of SM Higgs's coupling strength.

$c_{(\varphi/h)XX} =$	$C_{(\varphi/h)XX}/C_{hXX}^{(SM)}$
$c_{\varphi\bar{f}f}$	$s_\theta + \frac{6\xi\gamma c_\theta}{Z} + \frac{\gamma c_\theta}{Z}$
$c_{\varphi\gamma\gamma}$	$s_\theta + \frac{6\xi\gamma c_\theta}{Z} + \frac{\gamma c_\theta}{Z} - \gamma(b_2+b_Y)\frac{c_\theta}{Z}(F_1(\tau_W) + \frac{4}{3}F_{1/2}(\tau_t))^{-1}$
$c_{\varphi gg}$	$s_\theta + \frac{6\xi\gamma c_\theta}{Z} + \frac{\gamma c_\theta}{Z} - \gamma b_3\frac{c_\theta}{Z}(\frac{F_{1/2}(\tau_t)}{2})^{-1}$
$c_{\varphi W^+W^-}$	$s_\theta + \frac{6\xi\gamma c_\theta}{Z} + \frac{\gamma c_\theta}{Z}$
$c_{\varphi ZZ}$	$s_\theta + \frac{6\xi\gamma c_\theta}{Z} + \frac{\gamma c_\theta}{Z}$
$c_{h\bar{f}f}$	$c_\theta - s_\theta\frac{6\xi\gamma}{Z} - s_\theta\frac{\gamma}{Z}$
$c_{h\gamma\gamma}$	$c_\theta - s_\theta\frac{6\xi\gamma}{Z} - s_\theta\frac{\gamma}{Z} + \gamma(b_2+b_Y)\frac{s_\theta}{Z}(F_1(\tau_W) + \frac{4}{3}F_{1/2}(\tau_t))^{-1}$
c_{hgg}	$c_\theta - s_\theta\frac{6\xi\gamma}{Z} - s_\theta\frac{\gamma}{Z} + \gamma b_3\frac{s_\theta}{Z}(\frac{F_{1/2}(\tau_t)}{2})^{-1}$
$c_{hW^+W^-}$	$c_\theta - s_\theta\frac{6\xi\gamma}{Z} - s_\theta\frac{\gamma}{Z}$
c_{hZZ}	$c_\theta - s_\theta\frac{6\xi\gamma}{Z} - s_\theta\frac{\gamma}{Z}$

$$m_\varphi^2 = \frac{Z^2}{2}\left(M^2 - \sqrt{M^2 - \frac{4(1+6\gamma^2\xi)m_{\varphi_m}^2 m_{h_m}^2}{Z^2}}\right)$$
$$m_h^2 = \frac{Z^2}{2}\left(\frac{M^2 + \sqrt{M^2 - \frac{4(1+6\gamma^2\xi)m_{\varphi_m}^2 m_{h_m}^2}{Z^2}}}{(1+6\gamma^2\xi)}\right),$$

where $M^2 = m_{\varphi_m}^2 + m_{h_m}^2$ Thus, to keep m_φ and m_h (Lagrangian parameters) real, we must have

$$(m_{\varphi_m}^2 + m_{h_m}^2)^2 > \frac{4(1+6\gamma^2\xi)m_{\varphi_m}^2 m_{h_m}^2}{Z^2}.$$

For convenience, we drop the subscript and redefine φ_m and h_m as φ and h, respectively.

In our work, we assume that Λ_φ is greater than the vev of the SM Higgs and ξ is of order unity. Such a restriction is necessary as values greater than unity are not phenomenologically safe to consider because a large value can change the geometry itself through backreaction.

Next, we consider the effect of mixing on the coupling of the Higgs and radion to the various SM fields. We list and compare the coupling strength in the Table I in which the coupling of the radion to a pair of vector bosons also includes the trace anomaly term.

III. THEORETICAL AND EXPERIMENTAL CONSTRAINTS

With the radion-Higgs mixing discussed above, we constrain the model with the limits emanating from unitarity constraints and electroweak (EW) precision data. Similarities between the radion and the Higgs boson are utilized to

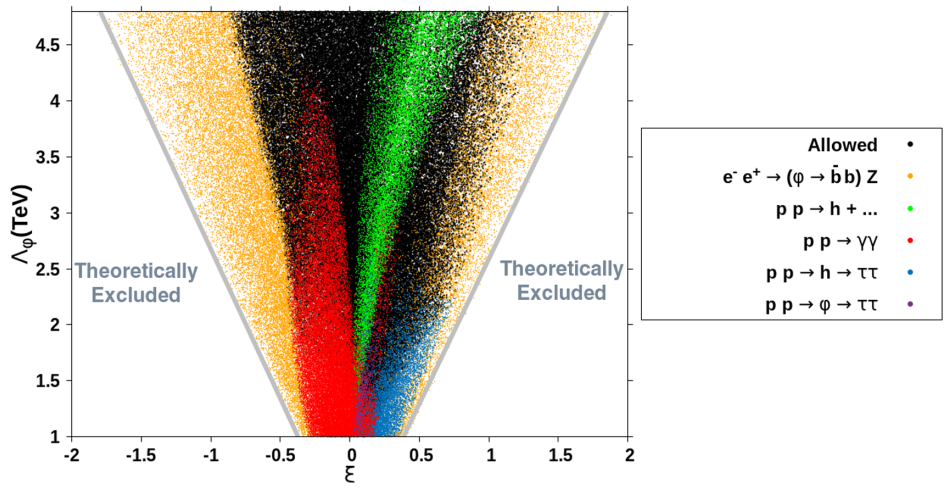

FIG. 1. Theoretically and phenomenologically excluded and allowed regions in the $\xi - \Lambda_\varphi$ plane obtained from LEP and LHC Higgs exclusion searches.

constrain the model further based on the bounds from Higgs exclusion searches and Higgs signal measurements:

(i) *Unitarity.*—It is well known that the Higgs boson plays a very crucial role in restoring the perturbative unitarity of gauge boson scattering in the SM. With the presence of another scalar in the theory with couplings similar to those of the Higgs boson, it becomes important to inquire if it ruins the perturbative unitarity of the theory. In fact, a lot of work has been done in this aspect of the radion [38–41], and it can be concluded that the contribution of a light radion with $\Lambda_\varphi \in [1:5]$ TeV to the amplitudes of these processes are subleading, and hence high-energy behavior is majorly decided by the SM Higgs boson.

(ii) *Electroweak precision data.*—The oblique parameters can be a useful way to constrain the effects of new physics, especially when the energy scale involved is close to $m_{Z/W}$. Since we consider a BSM scalar in this mass range, it becomes necessary to consider the constraints coming from these measurements [12,42]. Hence, analysis is made by ensuring that the parameter space satisfies the constraints emanating from EW precision measurements.

(iii) *Absence of graviton excitations.*—Current experimental limits from the LHC rule out any lowest graviton excitation of mass below 4.2 TeV for $k/M_5 \leq 0.1$ [43]. Using Eqs. (5) and (6), this limit translates to a lower bound on Λ_φ of a few TeVs. However, this bound can be relaxed considerably for models with more than one extra dimension [44–46]. In these classes of models, the mass of the graviton and its coupling to the SM fields are suppressed due to the presence of two scales in the theory, and Λ_φ as low as 1 TeV is allowed. In light of this discussion, this analysis has taken $\Lambda_\varphi \geq 1$ TeV.

(iv) *Tevatron, LEP, and LHC exclusion limits.*—Limits from the nonobservation of Higgs-like resonances at the Large Electron-Positron Collider (LEP), Tevatron, and LHC are imposed on this model through its implementation in HiggsBounds5.2.0 [47–49]. The HiggsBounds5.2.0 package is specifically designed to put bounds on different BSMs with an extended scalar sector, which in the case of the radion-Higgs mixing model consists of H, φ. It probes the modified scalar sector against the null results obtained from the LHC, LEP, and Tevatron due to the nonobservation of the Higgs boson, therefore putting exclusion bounds on the $\sigma \times$ branching ratio (BR) numbers in the respective decay channels at colliders. Those bounds translate to bounds on the parameter space while assuming that any of the scalar can be a Higgs boson of the SM, therefore requiring each of the scalars to evade the observation. To that end, the results are presented in Fig. 1.

The major constraint on the parameter space comes from the LEP process $e^- e^+ \to Zjj/b\bar{b}$ [50]. Because of the enhanced coupling of the φ to the gluon, $e^- e^+ \to Zjj/b\bar{b}$, puts the most stringent bound on

TABLE II. Best fit values of signal strengths (μ) along with 1σ uncertainties for various decay modes.

Signal strength μ_{XX}	$\sqrt{s} = 7$–8 TeV Table 13 in [51] $\mathcal{L} = 5$–20 fb^{-1}	$\sqrt{s} = 13$ TeV Table 2 in [2] $\mathcal{L} = 35.9$ fb^{-1}
$\mu_{\gamma\gamma}$	$1.14^{+0.19}_{-0.18}$	$1.20^{+0.18}_{-0.14}$
μ_{bb}	$0.70^{+0.29}_{-0.27}$	$1.12^{+0.29}_{-0.29}$
$\mu_{\tau\tau}$	$1.11^{+0.24}_{-0.22}$	$1.02^{+0.26}_{-0.24}$
μ_{WW}	$1.09^{+0.18}_{-0.16}$	$1.28^{+0.17}_{-0.16}$
μ_{ZZ}	$1.29^{+0.26}_{-0.23}$	$1.06^{+0.18}_{-0.18}$

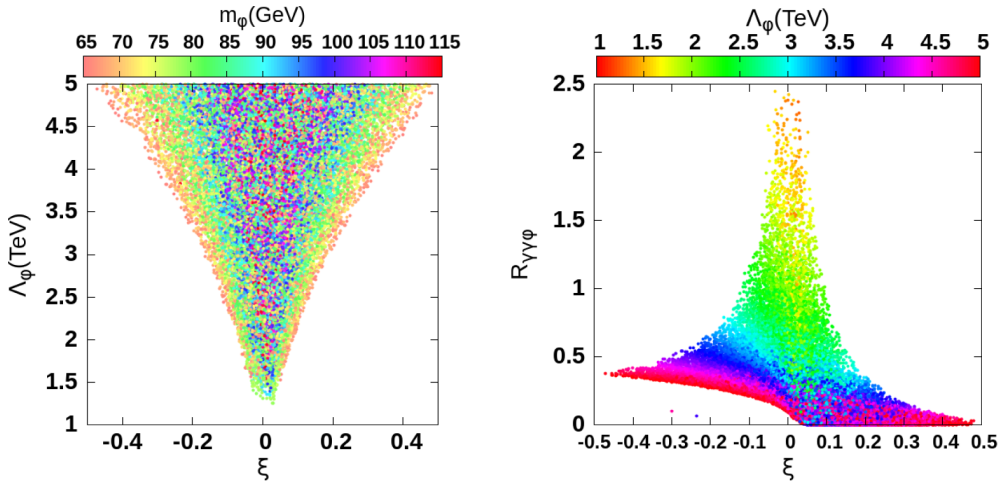

FIG. 2. Parameter space allowed from 2σ measurement of the μ parameter for $\gamma\gamma$, $\bar{b}b$, $\bar{\tau}\tau$, ZZ, W^-W^+ decay channels *(left)* and $R_{\gamma\gamma\varphi}$ values for that parameter space *(right)*.

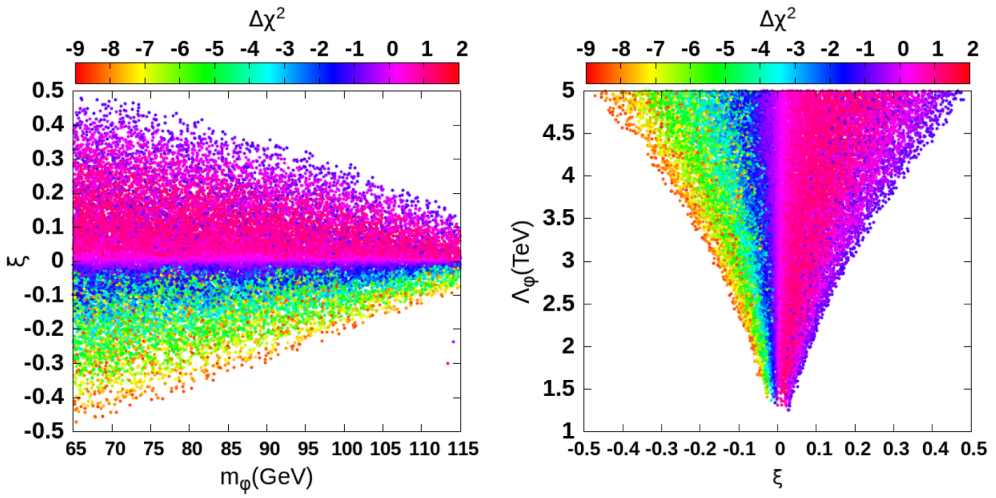

FIG. 3. The plot depicts $\xi - \Lambda_\varphi$ and $m_\varphi - \xi$ parameter space for different $\Delta\chi^2$ values. Note that $\Delta\chi^2 > 0$ signifies a better fit than that of the SM.

the allowed parameter space curtailing points at higher ξ for any Λ_φ. The LHC search for the SM Higgs before the Higgs discovery has resulted in the upper limits on the scalar production cross section as it restricts $\sigma(pp \to h)$ close to the SM values. In this model, the Higgs-like particle has an enhanced gluon coupling owing to its mixing with the radion in the $\xi > 0$ range, leading to enhanced gluon fusion production. Therefore, parts of the parameter space with positive ξ are ruled out. Because of the nonminimal contribution of the new radion mediated process $pp \to \varphi \to \gamma\gamma$ to the $pp \to \gamma\gamma$, which is aided by the enhanced gluon fusion production, the diphoton channel becomes one of the most sensitive channels. The same channel is also sensitive in the context of another hadronic machine, the Tevatron. However, because of the sheer scale of the LHC data (i.e., the LHC luminosity) compared to that from the Tevatron, the LHC constrains the parameter space of this model most.

(v) *Constraints from 125 GeV Higgs data*: Next, we analyze the constraints from the Higgs signal measurements. The current constraints on the Higgs signal which are given in terms of signal strengths (μ parameters) defined for various decay modes are shown in Table II. We have used these μ parameter values for decay modes $\gamma\gamma$, $\bar{b}b$, $\bar{\tau}\tau$, ZZ, W^-W^+ taken from the LHC data of $\sqrt{s} = 7$–8 TeV and luminosity 5 and 20 fb^{-1},[1] respectively [51]. The allowed

[1]Although $\sqrt{s} = 7$–8 TeV data are used for the analysis, we have also presented the final results with 13 TeV data as well, in Fig. 8, and found that the overall conclusion remains the same or fits even a bit better to the LHC data of 7–8 TeV.

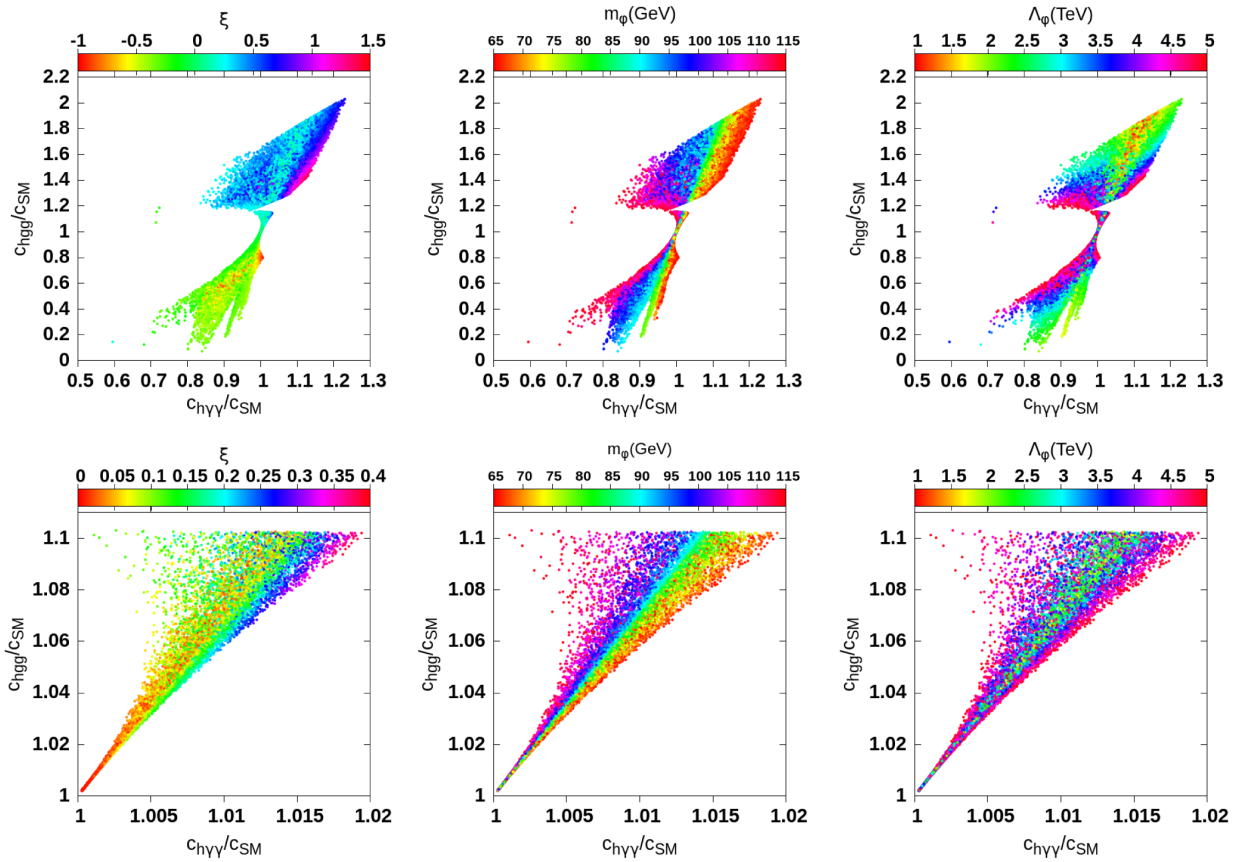

FIG. 4. The parameter space obtained using HiggsBounds (top) and requiring $\Delta\chi^2 > 0$ (bottom). $c_{\rm SM}$ is the corresponding coupling in the SM.

parameter space for the 2σ range of the Higgs signal measurements is presented in Fig. 2 (left). Later, we perform the χ^2 test to compare the mixed radion-Higgs scenario with the SM. The χ^2 is defined as

$$\chi^2 = \sum_i \frac{(\mu_{th} - \mu_i)^2}{\sigma_i^2}, \tag{18}$$

where μ_i is the μ parameter quoted above in the ith channel with 1σ error bar of σ_i and μ_{th} is the μ parameter calculated in the model. Using this definition, the modification in χ^2 compared to that of the SM is given as

$$\Delta\chi^2 = \chi^2_{\rm SM} - \chi^2_{\varphi h}, \tag{19}$$

where $\chi^2_{\varphi h}$ is the χ^2 calculated in the mixed radion-Higgs model.

To that end, we project samples on $\xi - \Lambda_\varphi$ and $\xi - m_\varphi$ plane for $\Delta\chi^2$ as shown in Fig. 3. It can be realized that the parameter region with $\xi > 0$ which corresponds to $\Delta\chi^2 > 0$ fits the LHC observations better than the SM Higgs. This is owed to the facts that positive ξ commensurate with the larger c_{hii} (where i denotes γ, g) and that pushes the μ parameter values to be greater than 1 in most of the Higgs decay channels as was quoted above. The correlation between c_{hgg} and $c_{h\gamma\gamma}$ for different parameters before and after imposing $\Delta\chi^2 > 0$ is compared in Fig. 4. It should be stressed that, in general, $c_{h\gamma\gamma}$ is more restricted than c_{hgg}. That is more so in the region where $\Delta\chi^2 > 0$, which restricts the $c_{h\gamma\gamma}$ close to the SM values while allowing a 10% increase for $c_{hgg}/c_{\rm SM}$ values. This indicates a slight increase of the Higgs production cross section in the gluon fusion channel, giving better fit than the SM.

IV. RESULTS AND DISCUSSION

A recent experimental observation in the light scalar sector is from the CMS [7] result that shows a small excess in the diphoton channel near the invariant mass of 95 GeV. This is the most recent in the variety of mild (less than or equal to 3σ) excesses that have been observed over last few years [4–6]. We first invoke the radion of the radion-Higgs mixing model as a light scalar that can potentially give rise to such a diphoton excess at different radion masses and later pin down the parameter space that explains the $\gamma\gamma$

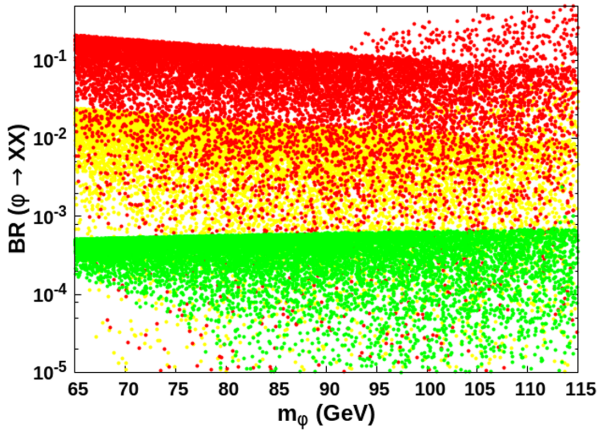

FIG. 5. This plot depicts branching ratios of the radion for a parameter space allowed from Higgs bound and Higgs signal results with a better fit to the LHC data than the SM Higgs, in a) the bb channel (yellow), b) the $\tau\tau$ channel (red), and c) the $\gamma\gamma$ channel (green).

channel excess at $m_\varphi \approx 95$ GeV. Similar to the SM Higgs, the radion is dominantly produced in the gluon fusion mode in this model, which is more prominent due to enhanced $c_{\varphi gg}$ coupling. This enhancement leads to a significant increase in the BR in the $\varphi \to gg$ mode, reducing the radion branching ratio into other final states. However, the drop in $\mathrm{BR}(\varphi \to \gamma\gamma)$ is minimal compared to the other channels. We present the radion branching ratio into different decay modes in Fig. 5. For a section of allowed points, the radion branching ratio to quark and lepton channels comes down significantly, pointing toward the utility of the $\gamma\gamma$ channel in the radion search at the LHC.

The ratio of the radion diphoton signal rate to that of the SM Higgs is defined as

$$R_{\gamma\gamma_{\varphi/h}} = \frac{\sigma(pp \to \varphi) \times \mathrm{BR}(\varphi \to \gamma\gamma)}{[\sigma(pp \to h) \times \mathrm{BR}(h \to \gamma\gamma)]_{\mathrm{SM}}}.$$

With the dominant production mechanism being the gluon fusion for both the SM Higgs and the radion, we rewrite the ratio as

$$R_{\gamma\gamma_{\varphi/h}} \approx \frac{\Gamma(\phi \to gg)}{\Gamma(h \to gg)_{\mathrm{SM}}} \times \frac{\mathrm{BR}(\varphi \to \gamma\gamma)}{\mathrm{BR}(h \to \gamma\gamma)_{\mathrm{SM}}}.$$

This ratio depicts the strength of the radion decay to the diphoton channel compared to that of the SM Higgs at respective masses. Here, we explore this ratio in two regions, namely, where a) the $\gamma\gamma$ cross section is well below the experimental observations as depicted by the black solid line in Fig. 6 and b) there is a significant possibility of observing a $\gamma\gamma$ excess for the points above the black line. A huge part of the parameter space is allowed from existing constraints such as the LHC, LEP, Tevatron exclusion bounds and LHC Higgs signal measurements with the Higgs-like scalar fitting the observations better than the SM Higgs ($\Delta\chi^2 > 0$). The allowed parameter region mainly leads to smaller $R_{\gamma\gamma\varphi}$ and is, therefore, also allowed from the light scalar search at the LHC. This part of the parameter space roughly corresponds to $\Lambda_\varphi > 2.5$ TeV. If we restrict our analysis to the points with $\Delta\chi^2 > 0$, the enhancement of the radion production cross section is significantly curtailed to limit itself to at most twice the SM number for a significant part of the parameter space. The advent of a dominant new decay mode in terms of $\varphi \to gg$ diminishes the $\varphi \to \gamma\gamma$ branching ratio significantly to restrict $R_{\gamma\gamma\varphi}$ to smaller values. For points with smaller positive ξ and smaller Λ_φ, we get some excesses in the diphoton channel for different radion masses. There is an indication of excess diphoton events around the 95 GeV radion mass, which was already hinted in CMS observation. The radion-Higgs mixing predicts toward a hint of radion diphoton rate enhancement at other masses like $m_\varphi \sim 70, 77, 90$ GeV as well. A future LHC light scalar search in the diphoton channel will either confirm the

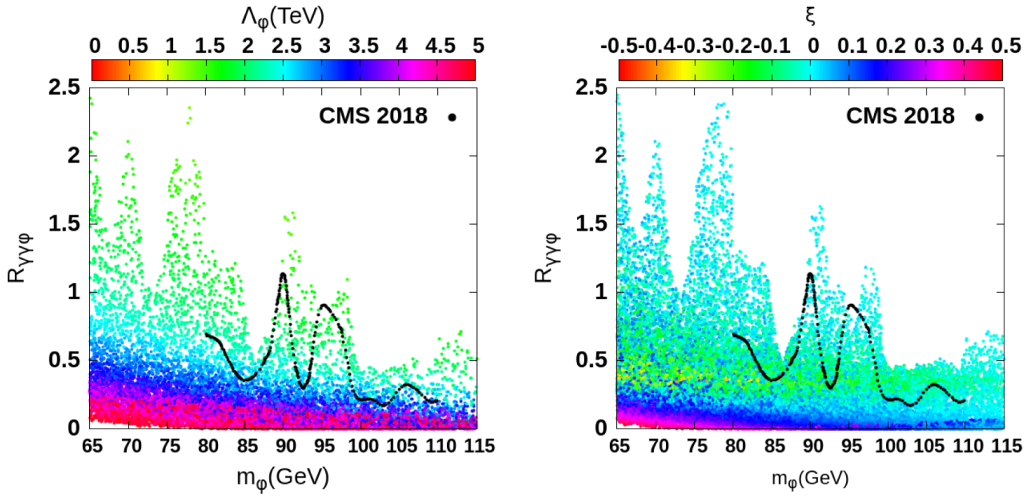

FIG. 6. Allowed parameter space for a better fit of the Higgs signal results than the SM.

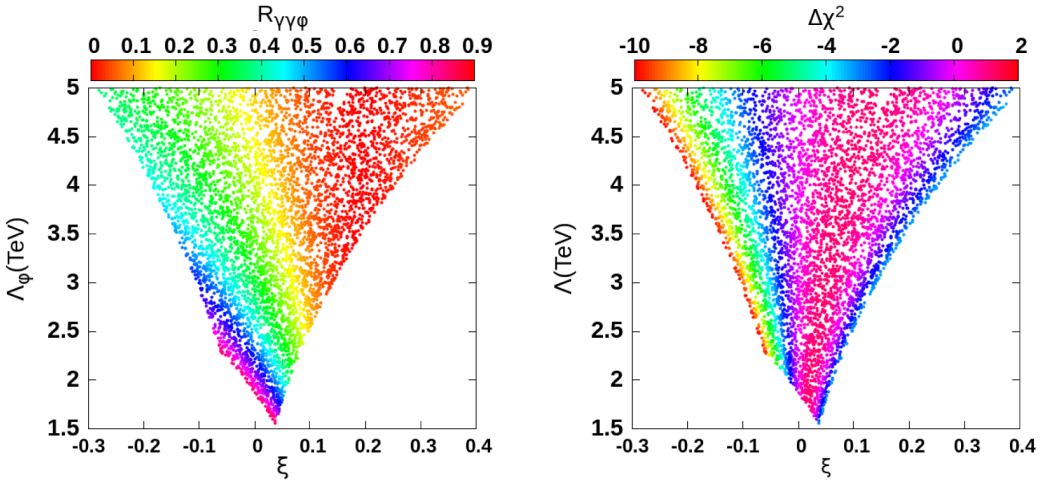

FIG. 7. $\xi - \Lambda_\varphi$ plane for different $\Delta\chi^2$ (left) and $R_{\gamma\gamma\varphi}$ values (right) at $m_\varphi = 95$ GeV and $\sqrt{s} = 7$–8 TeV.

presence of radion-borne excess or its absence will rule out that part of the parameter space that predicts these excesses.

We explore the parameter space for $m_\varphi = 95$ GeV further in Fig. 7. In words, $-0.25 \leq \xi \leq 0.35$ and 1.5 TeV $\leq \Lambda_\varphi \leq 5$ TeV satisfy all the theoretical and experimental constraints discussed above. For the central value of CMS excess at 95 GeV, $R_{\gamma\gamma\varphi}$ should be around 0.7. Table III shows a few points on the $\xi - \Lambda_\varphi$ plane obtained after requiring $\Delta\chi^2 > 0$ and $R_{\gamma\gamma\varphi} \sim 0.7$. It can be seen in Fig. 2 and Table III that 95 GeV anomaly can be explained even when $\xi \to 0$. However, it is evident in Fig: 7 that a nonzero positive mixing parameter ξ is necessary to obtain a better fit than the SM and explain the 95 GeV anomaly together. This is attributable to the discussed fact that $\xi > 0$ provides the required enhancement in various μ parameters, through an enhancement in the gluon-fusion production cross section. In Fig. 8, the results obtained using $\sqrt{s} = 13$ TeV data with 35.9 fb^{-1} luminosity are depicted. It can be observed that χ^2 improves for new data. This can be attributed mainly to the new μ parameter values obtained in the $b\bar{b}$ channel, which come closer to 1 compared to the earlier used value, therefore using the naturally arising μ parameter enhancement in the mixed radion-Higgs model.

To summarize, we have explored the Higgs radion model once again, to discuss the phenomenological prospects of the radion as a sub-125-GeV BSM scalar and its suitability to produce a diphoton excess at the LHC.

TABLE III. Coordinates on $\xi - \Lambda_\varphi$ plane for $\Delta\chi^2 > 0$ and $R_{\gamma\gamma\varphi} \sim 0.7$ satisfying all theoretical and experimental constraints.

ξ	Λ_φ (TeV)	$\Delta\chi^2$
0.0018	2.03	0.09
0.012	1.9	0.91
0.024	1.84	1.05
0.021	1.86	1.13
0.022	1.85	1.11

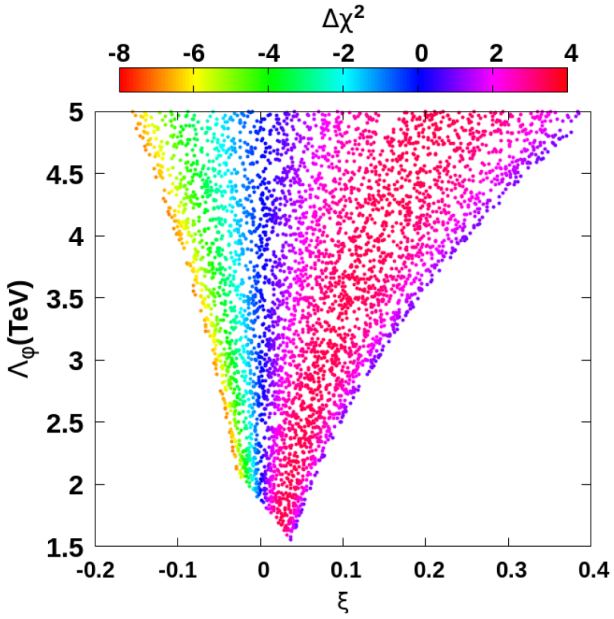

FIG. 8. $\xi - \Lambda_\varphi$ plane with varying $\Delta\chi^2$ at $m_\varphi = 95$ GeV and $\sqrt{s} = 13$ TeV.

Using HiggsBounds4, we obtain the parameter space that is allowed from the Higgs and new scalar search exclusion results from the LEP, Tevatron, and LHC together. The parameter space that is ruled out leads us to conclude that $e^+e^- \to Zh/\varphi$, $h/\varphi \to bb/jj$ is the most constraining for this model, with $pp \to \gamma\gamma$ and $pp \to h + X$ following the suit to exclude the model points. We also report that there is significant parameter space in this model where the Higgs-like scalar fits better with the LHC data than the SM Higgs. With a positive mixing parameter, i.e., $\xi > 0$, and being aided by the enhanced gluon fusion production rate, the Higgs-like scalar with a tinge of the radion is a more suitable candidate to be the observed 125 GeV scalar at the LHC.

ACKNOWLEDGMENTS

We would like to thank Debajyoti Choudhury for useful discussions and comments on the manuscript. D. S. would like to acknowledge financial supports through Ramanujan Fellowships of the Department of Science and Technology, Government of India. S. S. thanks UGC for the D. S. Kothari postdoctoral fellowship grant with award letter No. F.4-2/2006 (BSR)/PH/17-18/0126.

[1] ATLAS Collaboration, Combined Measurements of Higgs Boson Production and Decay Using up to 80 fb^{-1} of Proton–Proton Collision Data at $\sqrt{s} = 13$ TeV Collected with the ATLAS Experiment, Report No. ATLAS-CONF-2018-031, 2018.

[2] A. M. Sirunyan *et al.*, Combined measurements of Higgs boson couplings in proton–proton collisions at $\sqrt{s} = 13$ TeV, Eur. Phys. J. C **79**, 421 (2019).

[3] K. Cheung, J. S. Lee, and P.-Y. Tseng, New emerging results in higgs precision analysis updates 2018 after establishment of third-generation yukawa couplings, J. High Energy Phys. 09 (2018) 098.

[4] R. Barate *et al.*, Search for the standard model Higgs boson at LEP, Phys. Lett. B **565**, 61 (2003).

[5] A. M. Sirunyan *et al.*, Search for low mass vector resonances decaying into quark-antiquark pairs in proton-proton collisions at $\sqrt{s} = 13$ TeV, J. High Energy Phys. 01 (2018) 097.

[6] A. M. Sirunyan *et al.*, Search for resonances in the mass spectrum of muon pairs produced in association with b quark jets in proton-proton collisions at $\sqrt{s} = 8$ and 13 TeV, J. High Energy Phys. 11 (2018) 161.

[7] A. M. Sirunyan *et al.*, Search for a standard model-like Higgs boson in the mass range between 70 and 110 GeV in the diphoton final state in proton-proton collisions at $\sqrt{s} = 8$ and 13 TeV, Phys. Lett. B **793**, 320 (2019).

[8] D. Choudhury, A. Datta, and K. Huitu, ZZH coupling: A Probe to the origin of EWSB?, Nucl. Phys. **B673**, 385 (2003).

[9] W. D. Goldberger and M. B. Wise, Modulus Stabilization with Bulk Fields, Phys. Rev. Lett. **83**, 4922 (1999).

[10] O. DeWolfe, D. Z. Freedman, S. S. Gubser, and A. Karch, Modeling the fifth-dimension with scalars and gravity, Phys. Rev. D **62**, 046008 (2000).

[11] G. D. Kribs, TASI 2004 lectures on the phenomenology of extra dimensions, in Physics in $D \geqq 4$. *Proceedings, Theoretical Advanced Study Institute in Elementary Particle Physics, TASI 2004, Boulder, USA, 2004* (2006), pp. 633–699 [arXiv:hep-ph/0605325].

[12] C. Csaki, M. L. Graesser, and G. D. Kribs, Radion dynamics and electroweak physics, Phys. Rev. D **63**, 065002 (2001).

[13] N. Desai, U. Maitra, and B. Mukhopadhyaya, An updated analysis of radion-higgs mixing in the light of LHC data, J. High Energy Phys. 10 (2013) 093.

[14] E. E. Boos, V. E. Bunichev, M. A. Perfilov, M. N. Smolyakov, and I. P. Volobuev, Higgs-radion mixing in stabilized brane world models, Phys. Rev. D **92**, 095010 (2015).

[15] A. Chakraborty, U. Maitra, S. Raychaudhuri, and T. Samui, Mixed Higgs–radion states at the LHC—A detailed study, Nucl. Phys. **B922**, 41 (2017).

[16] R. Vega, R. Vega-Morales, and K. Xie, Light (and darkness) from a light hidden Higgs, J. High Energy Phys. 06 (2018) 137.

[17] D. Liu, J. Liu, C. E. M. Wagner, and X.-P. Wang, A light higgs at the LHC and the B-anomalies, J. High Energy Phys. 06 (2018) 150.

[18] J. H. Kim and I. M. Lewis, Loop induced single top partner production and decay at the LHC, J. High Energy Phys. 05 (2018) 095.

[19] L. Wang, X.-F. Han, and B. Zhu, Light scalar dark matter extension of the type-II two-Higgs-doublet model, Phys. Rev. D **98**, 035024 (2018).

[20] J. Cao, X. Guo, Y. He, P. Wu, and Y. Zhang, Diphoton signal of the light Higgs boson in natural NMSSM, Phys. Rev. D **95**, 116001 (2017).

[21] T. Biekötter, S. Heinemeyer, and C. Muñoz, Precise prediction for the Higgs-boson masses in the $\mu\nu$ SSM, Eur. Phys. J. C **78**, 504 (2018).

[22] U. Haisch and A. Malinauskas, Let there be light from a second light Higgs doublet, J. High Energy Phys. 03 (2018) 135.

[23] G. Cacciapaglia, G. Ferretti, T. Flacke, and H. Serodio, Revealing timid pseudo-scalars with taus at the LHC, Eur. Phys. J. C **78**, 724 (2018).

[24] P. J. Fox and N. Weiner, Light signals from a lighter higgs, J. High Energy Phys. 08 (2018) 025.

[25] F. Richard, Search for a light radion at HL-LHC and ILC250, arXiv:1712.06410.

[26] J.-Q. Tao *et al.*, Search for a lighter higgs boson in the next-to-minimal supersymmetric standard model, Chin. Phys. C **42**, 103107 (2018).

[27] R. Torre, Clockwork/Linear Dilaton: Structure and phenomenology, in *Proceedings, 53rd Rencontres de Moriond on Electroweak Interactions and Unified Theories (Moriond EW 2018): La Thuile, Italy* (2018), pp. 365–370 [arXiv:1806.04483].

[28] L. Liu, H. Qiao, K. Wang, and J. Zhu, A light scalar in the minimal dilaton model in light of lhc constraints, Chin. Phys. C **43**, 023104 (2019).

[29] T. Biekötter, M. Chakraborti, and S. Heinemeyer, An N2HDM solution for the possible 96 GeV excess, in *18th Hellenic School and Workshops on Elementary Particle Physics and Gravity (CORFU2018) Corfu, Corfu, Greece, 2018* (2019) [arXiv:1905.03280].

[30] K. Choi, S. H. Im, K. S. Jeong, and C. B. Park, A 96 GeV higgs boson in the general NMSSM, arXiv:1906.03389.

[31] J. M. Cline and T. Toma, Pseudo-Goldstone dark matter confronts cosmic ray and collider anomalies. Phys. Rev. D **100**, 035023 (2019).
[32] L. Randall and R. Sundrum, A Large Mass Hierarchy from a Small Extra Dimension, Phys. Rev. Lett. **83**, 3370 (1999).
[33] J. M. Cline and H. Firouzjahi, Brane world cosmology of modulus stabilization with a bulk scalar field, Phys. Rev. D **64**, 023505 (2001).
[34] D. Choudhury, D. P. Jatkar, U. Mahanta, and S. Sur, On stability of the three 3-brane model, J. High Energy Phys. 09 (2000) 021.
[35] S. Anand, D. Choudhury, A. A. Sen, and S. SenGupta, A geometric approach to modulus stabilization, Phys. Rev. D **92**, 026008 (2015).
[36] G. F. Giudice, R. Rattazzi, and J. D. Wells, Graviscalars from higher dimensional metrics and curvature Higgs mixing, Nucl. Phys. **B595**, 250 (2001).
[37] D. Dominici, B. Grzadkowski, J. F. Gunion, and M. Toharia, The Scalar sector of the Randall-Sundrum model, Nucl. Phys. **B671**, 243 (2003).
[38] U. Mahanta, Unitarity bound on the radion mass in the Randall-Sundrum model, arXiv:hep-ph/0004128.
[39] S. Bae, P. Ko, H. S. Lee, and J. Lee, Phenomenology of the radion in Randall-Sundrum scenario at colliders, Phys. Lett. B **487**, 299 (2000).
[40] D. Choudhury, S. R. Choudhury, A. Gupta, and N. Mahajan, Unitarity constraints on the stabilized Randall-Sundrum scenario, J. Phys. G **28**, 1191 (2002).
[41] T. Han, G. D. Kribs, and B. McElrath, Radion effects on unitarity in gauge boson scattering, Phys. Rev. D **64**, 076003 (2001).
[42] J. F. Gunion, M. Toharia, and J. D. Wells, Precision electroweak data and the mixed Radion-Higgs sector of warped extra dimensions, Phys. Lett. B **585**, 295 (2004).
[43] A. M Sirunyan *et al.*, Search for high-mass resonances in dilepton final states in proton-proton collisions at $\sqrt{s} = 13$ TeV, J. High Energy Phys. 06 (2018) 120.
[44] M. T. Arun and D. Choudhury, Bulk gauge and matter fields in nested warping: I. the formalism, J. High Energy Phys. 09 (2015) 202.
[45] M. T. Arun and D. Choudhury, Stabilization of moduli in spacetime with nested warping and the UED, Nucl. Phys. **B923**, 258 (2017).
[46] M. T. Arun and D. Choudhury, Bulk gauge and matter fields in nested warping: II. Symmetry Breaking and phenomenological consequences, J. High Energy Phys. 04 (2016) 133.
[47] P. Bechtle, O. Brein, S. Heinemeyer, G. Weiglein, and K. E. Williams, HiggsBounds: Confronting arbitrary higgs sectors with exclusion bounds from LEP and the tevatron, Comput. Phys. Commun. **181**, 138 (2010).
[48] P. Bechtle, O. Brein, S. Heinemeyer, O. Stål, T. Stefaniak, G. Weiglein, and K. E. Williams, HiggsBounds – 4: Improved tests of extended higgs sectors against exclusion bounds from LEP, the tevatron and the LHC. Eur. Phys. J. C **74**, 2693 (2014).
[49] P. Bechtle, S. Heinemeyer, O. Stal, T. Stefaniak, and G. Weiglein, Applying exclusion likelihoods from lhc searches to extended higgs sectors, Eur. Phys. J. C **75**, 421 (2015).
[50] E. Boos, S. Keizerov, E. Rahmetov, and K. Svirina, Higgs boson-radion similarity in production processes involving off-shell fermions, Phys. Rev. D **90**, 095026 (2014).
[51] G. Aad *et al.*, Measurements of the Higgs boson production and decay rates and constraints on its couplings from a combined ATLAS and CMS analysis of the LHC pp collision data at $\sqrt{s} = 7$ and 8 TeV. J. High Energy Phys. 08 (2016) 045.